Electronic Supplementary Material (ESI) for Inorganic Chemistry Frontiers.

Electronic Supplementary Information

Co_3O_4 Nanoparticles Supported on N-doped Electrospinning Carbon Nanofibers as an Efficient and Bifunctional Oxygen Electrocatalyst for Rechargeable Zn-Air Batteries

Liuzhe Qiu,[a] XiaopengHan,[*,a] Qi Lu,[a] Jun Zhao,[a] Yang Wang,[a] Zelin Chen[a], Cheng Zhong,[a] Wenbin Hu,[a,b] and Yida Deng[*,a]

[a]School of Materials Science and Engineering, Key Laboratory of Advanced Ceramics and Machining Technology of Ministry of Education, Tianjin Key Laboratory of Composite and Functional Materials, Tianjin University, Tianjin 300072, P.R. China.

[b]Joint School of National University of Singapore and Tianjin University, International Campus of Tianjin University, Binhai New City, Fuzhou 350207, China.

* Corresponding e-mail: xphan@tju.edu.cn; yida.deng@tju.edu.cn

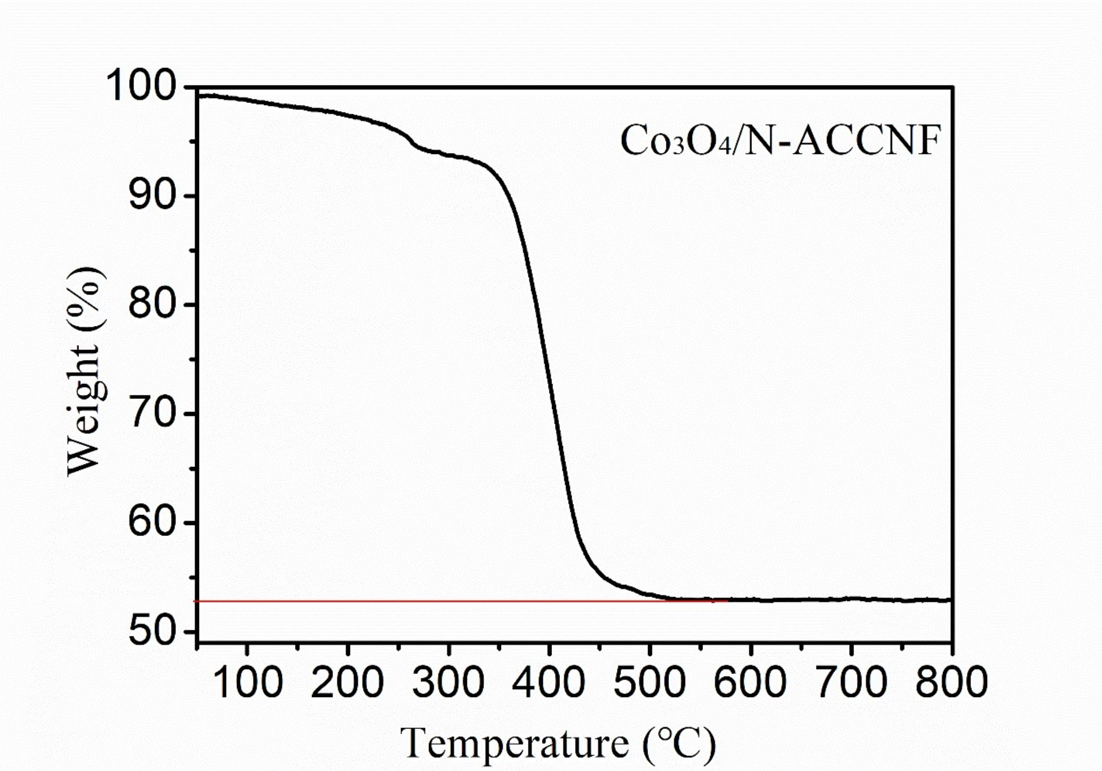

Fig. S1 Thermogravimetric curve of Co_3O_4/N-ACCNF tested in air atmosphere at a heating rate of 10 ºC min^{-1}.

A weight loss of about 5% below 250°C for the Co_3O_4/N-ACCNF is the evaporation of absorbed water. A weight loss of about 42% between 250 and 550 °C is indicative of a complete carbon oxidation in which a residual amount of about 53%, due to the composite cobalt oxide, indicate that the mass percentage of Co_3O_4 in the optimized Co_3O_4/N-ACCNF hybrid is 56% excluding the weight of the water.

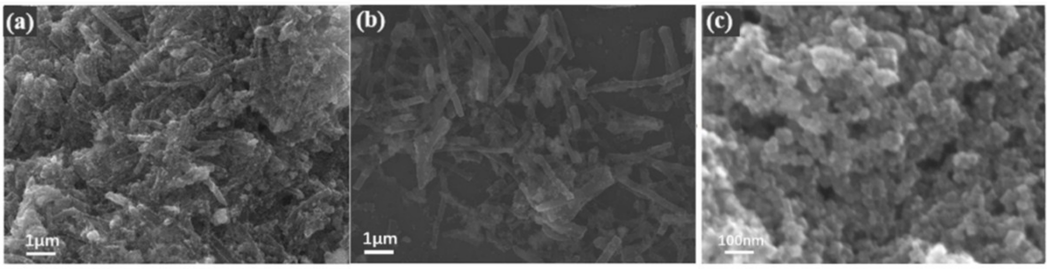

Fig. S2 SEM images of (a) Co_3O_4/N-ACCNF, (b) Co_3O_4/N-CNF, and (c) Co_3O_4 at low magnification.

.

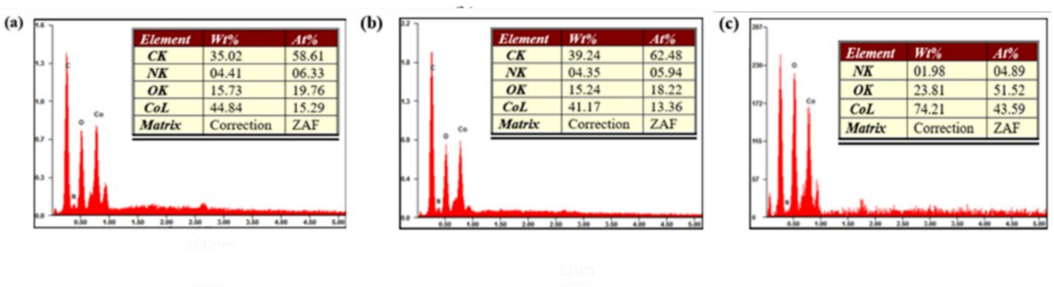

Fig. S3 SEM-EDS images of (a) Co_3O_4/N-ACCNF, (b) Co_3O_4/N-CNF, and (c) Co_3O_4.

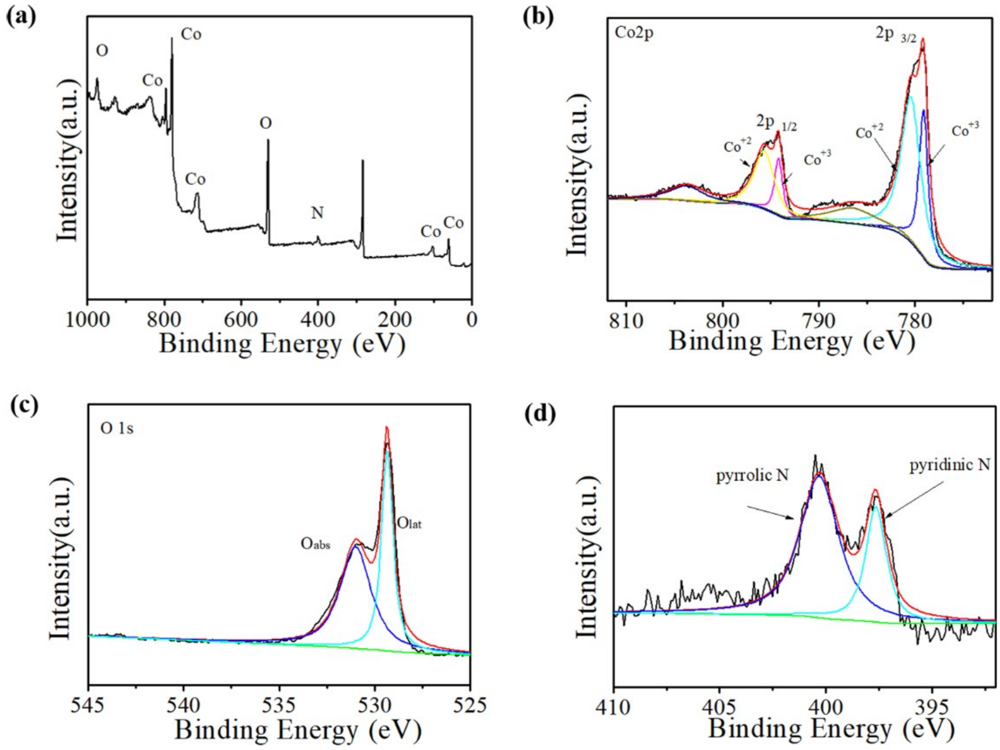

Fig. S4 (a) XPS survey spectrum, (b) Co2p, (c) O1s (d) N 1s of Co_3O_4-N/CNF.

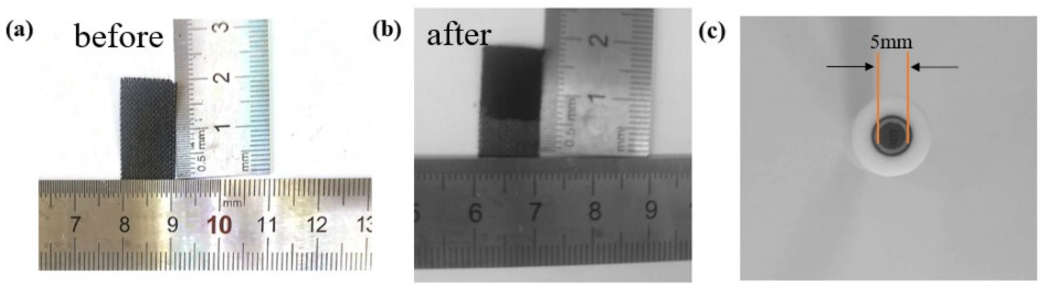

Fig. S5 Carbon cloth for OER electrochemical measurements: (a) before and (b) after and the RRED for ORR (c).

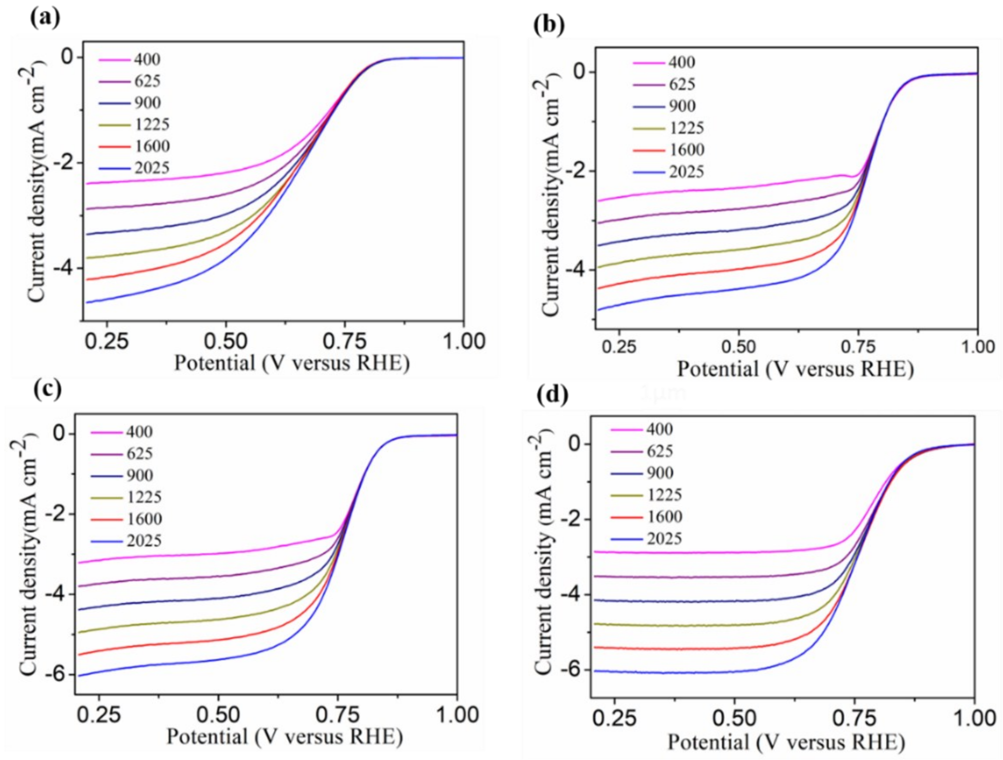

Fig. S6 Rotating-disk voltammograms at different rotation rates: (a) Co_3O_4/N-ACCNF, (b) Co_3O_4/N-CNF, (c) Co_3O_4, and (d) Pt/C.

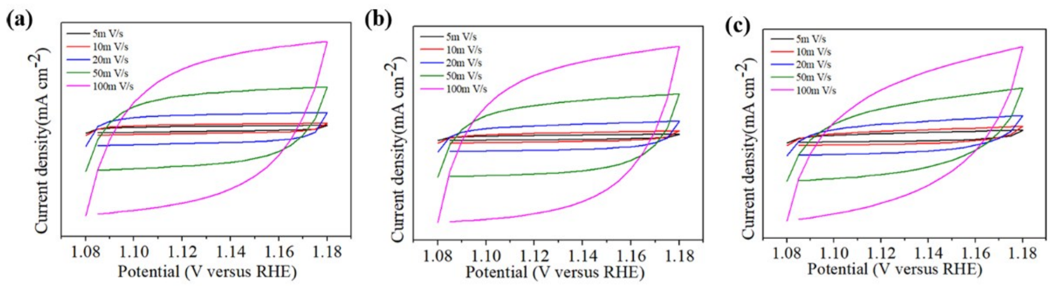

Fig. S7 Cyclic Voltammetry plots in the region of 0.05-0.15V vs SCE of (a) Co_3O_4/N-ACCNF, (b) Co_3O_4/N-CNF, and (c) Co_3O_4.

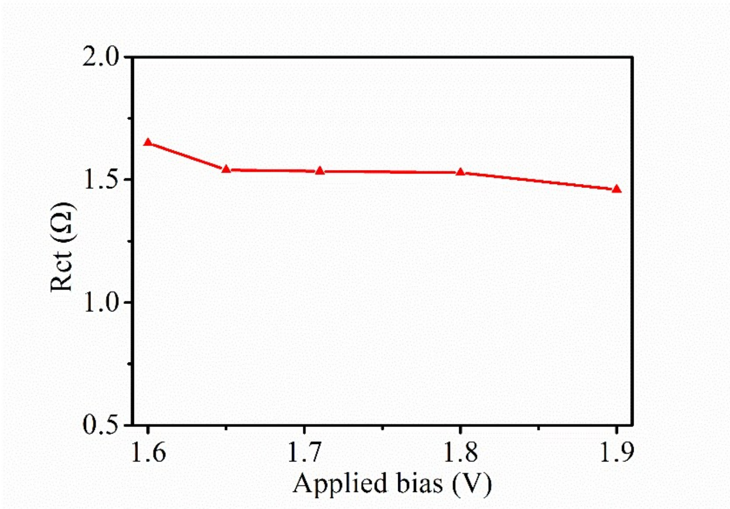

Fig. S8 Nyquist plots of Co_3O_4/N-ACCNF at different base of 1.60 V, 1.65 V, 1.71 V, 1.8V and 1.9V, extracted from impedance spectra measured with different applied bias. As show in Fig. S8, R_{ct} varies slightly with the different applied bias. In the entire range of applied bias, a slight decreased R_{ct} values were observed.

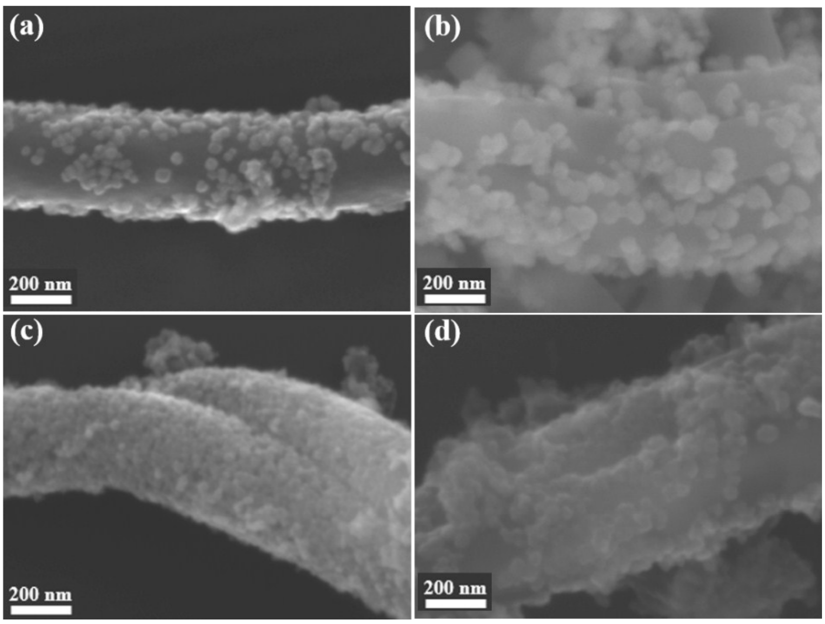

Fig. S9 SEM images of samples with different ACCNF addition amount: (a) 25mg, (b) 50 mg, (c) 75 mg and (d) 100 mg. In this experiment, the amount of loading Co_3O_4 particle can be adjusted by adjusting the addition amount of CNFs.

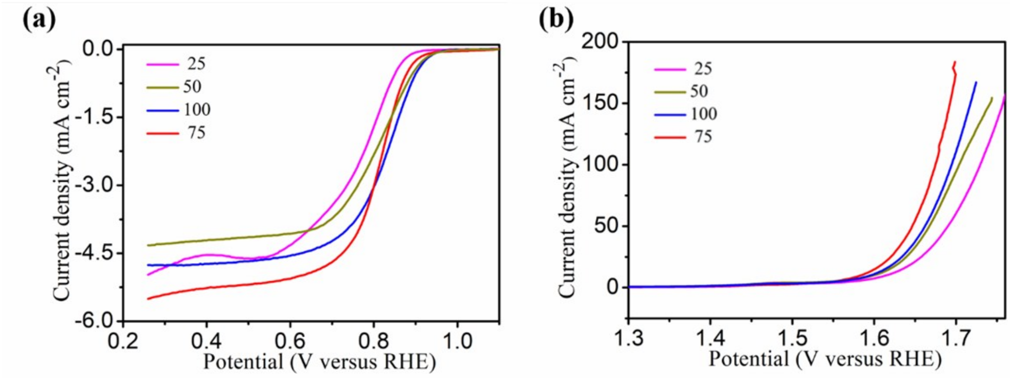

Fig. S10 (a) ORR and (b) OER activities of 25mg, 50 mg, 75 mg, 100 mg CNFs addition in Co_3O_4/N-ACCNF hybrid. SEM images show that, other conditions remain unchanged, when the added amount of CNFs is 75mg, LSV curves indicate that the sample with 75mg CNFs addition exhibits the best performance.

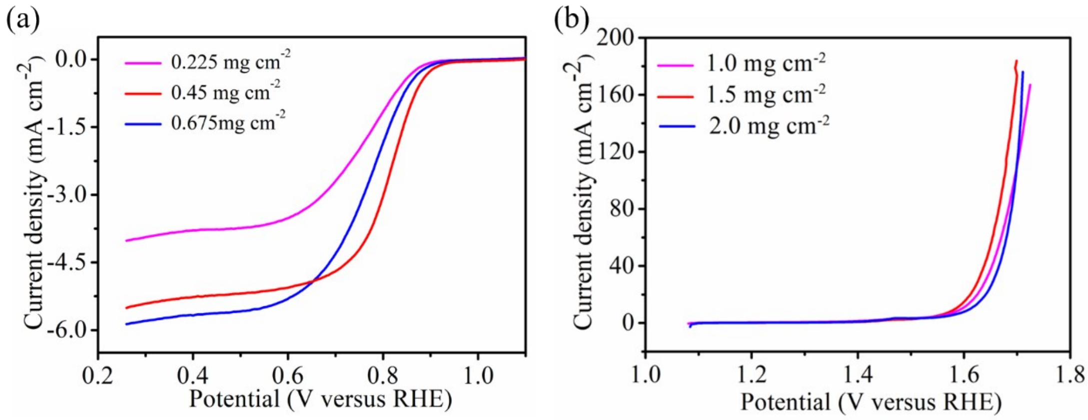

Fig. S11 (a) ORR and (b) OER activities of various catalyst mass loading of Co_3O_4/N-ACCNF hybrid.

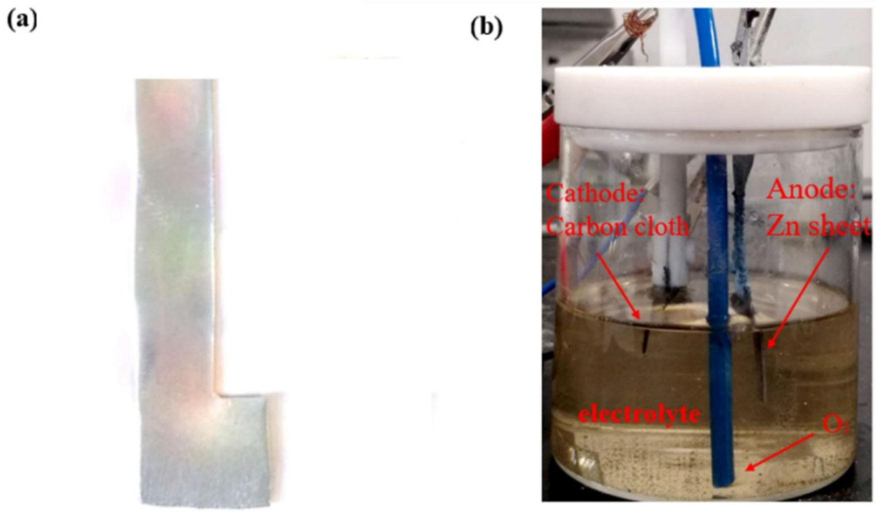

Fig. S12 (a) Polished zinc foil anode and (b) the assembled zinc-air battery device.

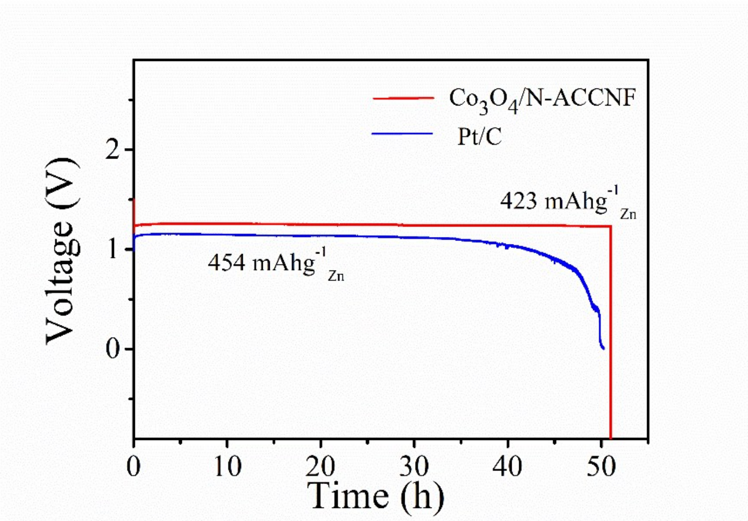

Fig. S13 Typical discharge curves of Co_3O_4/N-ACCNF and Pt/C-based ZABs at 10 mA cm^{-2}.

Table. S1 Summary of OER and ORR activities of synthesized catalysts.

Catalysts	OER Activity		ORR Activity			Overall evaluation
	Overpotential @10 mA cm^{-2} (V)	double layer capacitance (C_{dl})	Onset potential (V vs RHE)	Half-wave potential ($E_{1/2}$,V vs RHE)	Limiting current density (mA cm^{-2})	$\Delta E=E_{j=10}-E_{1/2}$ (V)
Co_3O_4-N/ACCNF	310	48.0	0.98	0.79	5.80	0.75
Co_3O_4-N/CNF	440	38.70	0.93	0.74	4.49	0.93
Co_3O_4	630	17.9	0.90	0.69	4.40	1.17
Pt/C	~	~	0.96	0.82	5.50	~
IrO_2	320	~	~	~	~	~

Table. S2 Comparison of electrocatalytic performances of Co_3O_4-N/ACCNF with other reported Co-based ORR electrocatalysts.

Catalyst	Electrolyte	Loading density (mg cm^{-2})	Current density (mA cm^{-2})	half-wavepotential (V)	Reference
Co_3O_4 nanoplates	0.1 M KOH	0.2	5.32	0.72	S1
$Co(OH)_2$ nanoplates	0.1 M KOH	0.2	5.24	0.69	S1
CoO_x/NG/g-C_3N_4	0.1 M KOH	0.16	4.9	0.794	S1
Co_3O_4@NMC	0.1 M KOH	0.408	~	0.833	S2
Co_3O_4/N-doped carbon	0.1 M KOH	0.86	2.15	0.95	S4
Co_3O_4 nanoparticles /N-doped	0.1 M KOH	1.0	5.95	0.86	S5
NCO-250	0.1 M KOH	0.149	5.31	0.75	S6
Co_3O_4-NP/N-rGO	0.1 M KOH	0.149	5.48	0.76	S7

Table. S3 Comparison of electrocatalytic performances of Co_3O_4-N/ACCNF with other reported Co-based OER electrocatalysts.

Catalysts	Support base	Electrolyte	Loading density (mg cm^{-2})	Overpotential at 10 mA cm^{-2}(mV)	Reference
Co_3O_4 nanoplates	GC	1 M KOH	0.2	390.1	S1
$Co(OH)_2$ nanoplates	GC	1 M KOH	0.2	396.0	S1
CoOx/NG/PCN	GC	0.1 M KOH	0.16	430.0	S2
Co_3O_4@NMC	Carbon cloth	0.1 M KOH	0.408	350.5	S3
NCO-250	GC	1 M KOH	0.149	320	S6
Co_3O_4-NP/N-rGO	GC	1 M KOH	0.15	380	S7
Co_3O_4-N/ACCNF	Carbon cloth	1 M KOH	1.5	310	This work

Table. S4 Comparison of the bifunctional activity of Co_3O_4-N/ACCNF with previously reported transition metal-based materials.

Catalysts	OER Activity		ORR Activity		Overall evaluation	Reference
	Overpotential @10 mA cm^{-2} (V)	double layer capacitance (C_{dl})	Half-wave potential ($E_{1/2}$,V vs RHE)	Limiting current density (mA cm^{-2})	$\Delta E=E_{j=10}-E_{1/2}$ (V)	
Co_3O_4-N/ACCNF	310	48.0	0.79	5.80	0.75	This work
Co_2Ni_1@NC	300	11	0.76	4.05	0.77	S8
(Ni,Co)/CNT	N.A.	~	0.74	5	0.87	S9
NC- Co_3O_4/CC	352	~	0.87	12.82	0.71	S10
CMN-231 nanorods	401	~	0.749 V	6	0.88 V	S11
Co–CeO_2–N–C	326	41.0	0.82	3.8	0.74	S12
N-NiO	270	28.4	0.69	3.4	0.83	S13
Mn/Co–N–C	430	6.32	0.8	5.1	0.76	S14

References

S1 P. Tan, Z Wu, B. Chen, H. Xu, W. Cai, M. Ni, *Electrochim. Acta.,*2019, **310,** 86-95.

S2 W. Chen, L. Ge, L, Ding, Y. Xu, F. You, K. Wang, *J. Alloy Compd.* 2019, **789,** 874-880.

S3 Y. Wang, X. Xu, L. Liu, J. Chen, G. Shi, *Dalton transactions,* 2019, **48,** 7150-7157.

S4 B. Wang, L. Xu, G. Liu, P. Zhang, W. Zhu, J. Xia, H. Li, *J. Mater. Chem. A.,* 2017, **5,** 20170-20179.

S5 Z. Liu, Q. Su, P. Diao, F. Li, *Chemelectrochem,* 2017, **4,** 2260-2268.

S6 J. Zhao, J, Y. He, Z. Chen, X. Zheng, X. Han, D. Rao, C. Zhong, W. Hu, Y. Deng, *ACS Appl. Mater. Interfaces* 2019, **11,** 4915-4921.

S7 X. Han, G. He, Y. He, J. Zhang, X. Zheng, L. Li, C. Zhong, W. Hu, Y. Deng and T.-Y. Ma, *Adv. Energy Mater.*, 2018, **8**, 1702222.

S8 J. Ran, X. Guo, P. Liu, S. Peng, X. Gao and D. Gao, *Nanotechnology,* 2019, **30**.

S9 N. Ma.; Y. Jia.; X. F. Yang.; X. L. She.; L. Z. Zhang.; Z. Peng.; X. D. Yao.; D. J. Yang. *J. Mater. Chem.* A 2016, **4**, 6376-6384.

S10 Guan, C.; Sumboja, A.; Wu, H.; Ren, W.; Liu, X.; Zhang, H.; Liu, Z.; Cheng, C.; Pennycook, S. J.; Wang, J. Hollow. *Adv. Mater.* 2017, **29**, 1704117.

S11 Q. Wang, Y. Xue, S. Sun, S. Yan, H. Miao and Z. Liu, *J Power Sources*, 2019, **435**.

S12 Z. Zhang, D. Gao, D. Xue, Y. Liu, P. Liu, J. Zhang and J. Qian, *Nanotechnology,* 2019, **30**

S13 C. Li, Z. Yu, H. Liu and M. Xiong, *Chem Eng J,* 2019, **371**, 433-442.

S14 L. Wei, L. Qiu, Y. Liu, J. Zhang, D. Yuan and L. Wang, *Acs Sustain Chem Eng*, 2019, **7,** 14180-14188.